NASA TECHNICAL MEMORANDUM

NASA TM X- 73995

NASA TM X- 73995

THE PHOTOMETRY OF FLAT, BASALTIC SURFACES

W. R. Weaver and W. E. Meador
Langley Research Center

January 1977

NASA
National Aeronautics and Space Administration

Langley Research Center
Hampton, Virginia 23665

1. Report No.	2. Government Accession No.	3. Recipient's Catalog No.
NASA TM X-73995		

4. Title and Subtitle	5. Report Date
THE PHOTOMETRY OF FLAT, BASALTIC SURFACES	January 1977
	6. Performing Organization Code 64.600
7. Author(s) W. R. Weaver and W. E. Meador	8. Performing Organization Report No.
	10. Work Unit No. 185-50-51-01
9. Performing Organization Name and Address NASA Langley Research Center Hampton, Virginia 23665	11. Contract or Grant No.
	13. Type of Report and Period Covered Technical Memorandum
12. Sponsoring Agency Name and Address National Aeronautics and Space Administration Washington, DC 20546	14. Sponsoring Agency Code

15. Supplementary Notes

Interim technical information release, subject to possible revision and/or later formal publication.

16. Abstract

A photometer was developed and successfully operated to obtain photometric measurements on several flat, particulate surfaces of basalt for coplanar scattering geometries. The test materials were two size ranges each of two different basalts with significantly different albedos. The measurements include a range of phase angles from 30 to 80 degrees and were obtained by varying the angles of incidence and emission such that the phase angle remained constant. The data were used elsewhere in the verification of the Meador-Weaver photometric function and are presented here in the form of Minnaert plots. In this form the data offered the first support for the accuracy of the Meador-Weaver photometric function because of a deviation of the data from a straight line trend at larger departures from the mirror point geometry. This trend is predicted by the Meador-Weaver function but not by the Minnaert function. The failure of photometric data to support the Minnaert function was not evident in earlier measurements because of the restriction of planetary data to small departures from the mirror point geometry and to small values of the phase angle.

17. Key Words (Suggested by Author(s)) (STAR category underlined)	18. Distribution Statement
Photometry, apparatus Photometric function Photometry of flat, particulate surfaces Optics (STAR Cat. 74)	Unclassified - Unlimited

19. Security Classif. (of this report)	20. Security Classif. (of this page)	21. No. of Pages	22. Price*
Unclassified	Unclassified	34	$4.00

*Available from The National Technical Information Service, Springfield, Virginia 22161

THE PHOTOMETRY OF FLAT, BASALTIC SURFACES

W. R. Weaver and W. E. Meador
Langley Research Center

SUMMARY

A photometer was developed and successfully operated to obtain photometric measurements on several flat, particulate surfaces of basalt for coplanar scattering geometries. The test materials were two size ranges each of two different basalts with significantly different albedos. The measurements include a range of phase angles from 30 to 80 degrees and were obtained by varying the angles of incidence and emission, such that the phase angle remained constant. The data were used elsewhere in the verification of the Meador-Weaver photometric function and are presented here in the form of Minnaert plots. In this form the data offered the first support for the accuracy of the Meador-Weaver photometric function because of a deviation of the data from a straight line trend at larger departures from the mirror point geometry. This trend is predicted by the Meador-Weaver function but not by the Minnaert function. The failure of photometric data to support the Minnaert function was not evident in earlier measurements because of the restriction of planetary data to small departures from the mirror point geometry and to small values of the phase angle.

INTRODUCTION

The importance of photometry in the remote sensing of planetary surfaces is its potential for describing the brightness of a surface in reflected sunlight as a function not only of the angles of incidence, emission, and phase, but also as a function of the physical properties of the surface material.

This potential has not been fully realized, however, because of the prevalence of photometric functions that are highly empirical. One such function, the Minnaert (ref. 1), is the most commonly used for correlating and analyzing data from planetary surfaces and for describing the reflectance from planetary surfaces. (See for example refs. 2, 3, and 4.) The Minnaert function, however, has little basis in theory and, therefore, cannot be used to interpret photometric behavior in terms of the physical properties of the reflecting surface.

Reference 5 reports the development of a new generalized photometric function for particulate surfaces that significantly enhances the potential of photometry by allowing at least qualitative predictions of surface properties from the measurement of reflected visible radiation. The development and verification of this function required photometric data for a range of scattering geometries for surfaces of different particle sizes and albedos. Adequate data were not available, so a photometer was developed and successfully used for the photometric measurements. This paper reports the details of the photometer, the test materials, and the photometric data used in the development and verification of the photometric function of reference 5 because it offers experimental support for certain characteristics of the function and it offers researchers photometric data that covers a range of geometries, particle sizes, and particulate materials.

SYMBOLS

a_0, a_1, a_2	empirical parameters in equation (2)
B	measured surface brightness (arbitrary units)
B_0	parameter in equation (1)
E	emission angle (see fig. 1)
f	shadowing-correction factor (see eq. (3))

I	incidence angle (see fig. 1)
k	Minnaert exponent (see eq. (1))
x	integration variable (see eq. (3))
α	phase angle (see fig. 1)
μ	function defined by equation (4)
ν	function defined by equation (5)
Φ	surface brightness normalized to unity at $I = E = 0$

PHOTOMETRIC FUNCTIONS

The most commonly used photometric function for correlating and analyzing data of planetary surfaces and for describing the reflection from (or brightness of) planetary surfaces is the well-known Minnaert function (ref. 1). The Minnaert function is

$$\Phi(I,E,\alpha) = B_0(\alpha)(\cos I)^{k(\alpha)}(\cos E)^{k(\alpha)-1} \qquad (1)$$

where $\Phi(I,E,\alpha)$ is the brightness (normalized to unity at $I = E = 0$) and the angles of incidence (I), emission (E), and phase (α) are related according to figure 1. It is simply Lambert's Law for diffuse reflection modified in accordance with the reciprocity principle. As such, it is highly empirical with little basis in theory and, of considerable importance, it cannot be used to interpret photometric behavior in terms of the physical properties of the reflecting surface.

The photometric function developed by Meador and Weaver (ref. 5) contrasts considerably with the Minnaert function. The Meador-Weaver function has basis in theory, has been verified for several materials in laboratory experiments, and has been used to predict some characteristics of the surface of Mars that are in qualitative agreement with existing models of the surface (refs. 6 and 7).

The function is applicable to all geometries of scattering, it takes into account single scattering, multiple scattering, and interparticle shadowing and it also contains parameters, the values of which depend on the physical properties of the surface. The Meador-Weaver function of reference 5 is

$$\Phi(I,E,\alpha) = \frac{\cos I}{(1 + a_0 + a_1)(\cos I + \cos E)} [(1 + a_0 \cos \alpha)\ f\ (I,E,\alpha,a_2) + a_1(\cos I + \cos E)] \tag{2}$$

The empirical parameters a_0, a_1, and a_2 contain information about characteristics of the particulate surface such as particle size, single-particle albedo, and compactness, and the factor $f(I,E,\alpha;a_2)$, the shadowing-correction factor, is given by

$$f(I,E,\alpha,a_2) = e^{\mu-\nu} + \nu \int_0^1 \exp\left\{\mu - \frac{\nu}{6\pi}\left[3\pi x + 2(2 + x^2)(1 - x^2)^{1/2} + 6x \sin^{-1}x\right]\right\} dx \tag{3}$$

where

$$\mu = \frac{4a_2(1 + \cos \alpha)}{3 \sin \alpha} \tag{4}$$

and

$$\nu = \frac{\pi a_2(\cos I + \cos E)}{\sin \alpha \cos I \cos E}\left[\sin^2 \alpha + 2(1 + \cos \alpha) \cos I \cos E\right]^{1/2} \tag{5}$$

Reference 5 points out that an improper behavior of equation (3) near grazing incidence or emission can be corrected by using equation (3) for all scattering geometries for which f exceeds unity, and replace equation (3) with $f = 1$ for larger values of incidence or emission.

THE PHOTOMETER

The photometer that was successfully used to make the measurements which formed a basis for the development and verification of the Meador-Weaver photometric function is shown in figure 2 and consists of a 7.6-cm-diameter pipe formed into a semicircular guide 3.7 m in diameter, and two 61-cm-diameter parabolic mirrors which clamp to the guide. The guide is calibrated in 2.5 degree increments and the movement of the mirrors along the guide is aided by polytetrafluorethylene inserts in the clamps. Each mirror has a fine screw adjustment in the vertical plane and pointers that project a narrow beam of light. This allows the precise pointing of the mirrors at the center of the scattering surface thus compensating for any inaccuracies in the shape of the semicircular guide and greatly improving the accuracy of the angular settings of the mirrors. The calibrated guide to the left of the main guide in figure 2 is movable and pivots about the normal to the center of the scattering surface and permits measurements for geometries in which the surface normal is not in the scattering plane. Although the use of large mirrors prohibits measurements at phase angles smaller than 30 degrees, the large illuminated areas permit the study of the photometric effects of rough surface topographies which are more difficult to represent on a smaller scale.

The source mirror has a high-pressure, short-arc mercury lamp mounted at the focal point of its parabolic contour (focal length = 24.6 cm). The lamp is housed in a small metal enclosure (2.5 cm by 10.2 cm) only slightly larger than the lamp itself to protect against explosion of the quartz envelope and to prevent direct illumination of the test surface. The lamp is cooled by high-pressure air fed through the small tube which can be seen to the left of figure 3, a photograph of the source mirror. The lamp housing is supported by

a current-carrying rod attached to the center of the mirror and positioned by four wires attached to the mirror's periphery. The lamp is adjusted to the focal point by imaging the beam at about 10 m and adjusting the length of the supporting rod and the four supporting wires until the beam is uniform and the same diameter as the mirror. The result is a very small beam divergence angle and an accurate positioning of the lamp. The two light beam pointers used to aim the mirror precisely at the center of the test surface can be seen in figure 3 mounted on each side of the mirror. The uniformity of the light beam was measured at the distance of the test surface and is shown in figure 4.

Figure 5 shows the details of the parabolic detector mirror that collects the scattered light and focuses it on a silicon-diffused guard ring photodiode mounted at the focal point (focal length = 24.6 cm). The diode is supported by a metal, wire-carrying tube and is positioned by four wires attached to the mirror's periphery. The positioning of the diode at the focal point was accomplished by facing the two mirrors toward each other, accurately alining their axes, substituting a blackened metal disk for the anode, and (with the lamp operating) adjusting the diode holder until the smallest, most-well-defined spot was obtained at the point on the substitute diode that simulated the active area of the actual diode.

TEST MATERIALS

Photometric data were taken on two materials: a Colorado basalt and a basalt dune sand. The Colorado basalt is from the intrusive and hypabyssal rocks occurring in the Ralston intrusives region of Colorado and has been characterized by J. Gliozzi of Martin Marietta Aerospace as a "mafic latite porphyry (mafic trachyandesite porphyry)." Larger rocks were crushed to

produce a powder that is light brown in color and has an albedo of about 0.4. Table I gives a chemical analysis of the igneous rocks found in the same area as the test material.

The basalt dune sand is a well sorted sand from a small area of active dunes about 25 km east of Flagstaff, Arizona, in the eastern part of the San Francisco volcanic field. The dune sand has accumulated in the lee of a basaltic lava flow from Maroon Crater and is believed by E. W. Wolfe of the U. S. Geologic Survey "to represent the fine-grained material transported by the wind from the surface of the widespread airfall cinder sheet deposited in the eruption of Sunset Crater, which is located about 16 km to the northwest of the dune." The material was used unaltered; it is black in color, and has an albedo of less than 0.1. Table II gives a representative chemical analysis of the dune material. Figures 6 and 7 are photographs made with an electron beam microscope of the Colorado basalt and the basalt dune sand, respectively, and show several particles enlarged 55 times and a single particle enlarged 550 times.

Each material was mechanically sieved into two particle size ranges and figure 8 gives the particle size distribution of the test materials obtained on an optical particle analysis system. Because of the large amount of extremely small, adhesive fines of the Colorado basalt, it was sieved with a water wash, whereas, the basalt dune sand was free of very small fines and was not washed.

TEST PROCEDURES

The test surface is contained in a 1.5-m-diameter pan which can be rotated about its center. Loosely packed, optically thick (at least five particle

diameters) test surfaces were formed by sifting the test material upon flat base layers of the same material. The base layer was made flat by sliding across the material a heavy metallic bar that moved along two polytetrafluoroethylene rods mounted on the floor at each side of the pan. After a test surface was prepared, the source and detector mirrors were positioned, and the pan rotated while the reflected light was measured. This was repeated for several mirror positions and if little change was noted in the detector output as the pan was rotated, the surface was considered photometrically flat and uniform.

Photometric measurements were made for coplanar scattering geometries as the two mirrors were moved in unison (2.5-degree steps) along the supporting guide and thereby the angles of incidence and emission were changed, while the phase angle was held constant. Sets of measurements on each of the four laboratory materials (namely, two particle-size ranges for each of the basalts) were obtained in this manner for 11 values of the phase angle from 30 to 80 degrees in 5-degree steps. For each data set the initial value of the incidence angle (also, the largest value) was 75 degrees and no data were taken for emission angles larger than 75 degrees.

RESULTS

The photometric measurements made on the four basalt test surfaces are presented in figures 9 through 12 in the form of Minnaert plots which plot log (B cos E) against log (cos I cos E) for fixed values of the phase angle where B is the measured brightness. This format is widely used for correlating numerous brightness measurements and derives from the particular form of the Minnaert photometric function (eq. (1)) which predicts straight lines for such plots. The data for the four surfaces are not referenced to a single

photometric standard, but the data for an individual test surface were taken at a fixed set of conditions for the source and the detector.

Figures 9 through 12 show the data to have a characteristic linear trend starting near the mirror point (incidence angle = emission angle) at the extreme right in each plot and continuing to the left as log (cos I cos E) decreases, then the data falls below a straight-line extension. This behavior is better illustrated by figures 13 and 14 which show on a larger scale the measured photometric data for the four test surfaces at a phase angle of 30 degrees, together with a straight line for comparison. These figures clearly show the initial linearity near the mirror point and the later deviation from linearity at decreasing values of log (cos I cos E) for each of the test surfaces.

The deviation from linearity (i.e., a variation in k of eq. (1)) with decreasing values of log (cos I cos E) does not support the form of the Minnaert function (eq. (1)). It is, however, the precise behavior predicted in reference 5 for the Meador-Weaver function. Thus, the photometric measurements of figures 9 through 12 offered the first experimental verification that the Meador-Weaver function is a valid generalization of the Minnaert function. The lack of support for the Minnaert function indicated by the present data does not necessarily conflict with the data of previous work used to support that function. Previous planetary measurements have not been extended to very large departures from the mirror point geometry or to large phase angles (see, for example, refs. 2 and 3) except for the work of reference 4, which presents too few data points with too much scatter to make a definitive judgment about the behavior at large deviations from the mirror geometry. Therefore, nonlinear

parts of Minnaert plots may well exist without contradicting the available experimental evidence.

CONCLUDING REMARKS

A photometer was developed and successfully operated to obtain photometric measurements on several flat, particulate surfaces of basalt for coplanar scattering geometries. The test materials were two size ranges each of two different basalts with significantly different albedos. The measurements include a range of phase angles from 30 to 80 degrees and were obtained by varying the angles of incidence and emission such that the phase angle remained constant. The data are that used in the verification of the Meador-Weaver photometric function and are presented in the form of Minnaert plots. In this form the data offered the first support for the accuracy of the Meador-Weaver photometric function because of a deviation of the data from a straight line trend at larger departures from the mirror point geometry. This trend is predicted by the Meador-Weaver function but not by the Minnaert function. That this failure of photometric data to support the Minnaert function was not evident in earlier measurements is due to the restriction of planetary data to small departures from the mirror point geometry and to small values of the phase angle.

REFERENCES

1. Minnaert, M.: The Reciprocity Principle in Lunar Photometry. Astrophys. J., vol. 93, no. 3, May 1941, pp. 403-410.
2. Young, A. T.; and Collins, S. A.: Photometric Properties of the Mariner Cameras and of Selected Regions on Mars. J. Geophys. Res., vol. 76, no. 2, Jan. 10, 1971, pp. 432-437.

3. Binder, Alan B.; and Jones, J. Colin: Spectrophotometric Studies of the Photometric Function, Composition, and Distribution of the Surface Materials of Mars. J. Geophys. Res., vol. 77, no. 17, June 10, 1972, pp. 3005-3020.

4. Thorpe, Thomas E.: Mariner 9 Photometric Observations of Mars From November 1971 Through March 1972. Icarus, vol. 20, no. 4, Dec. 1973, pp. 482-489.

5. Meador, W. E.; and Weaver, W. R.: A Photometric Function for Diffuse Reflection by Particulate Materials. NASA TN D-7903, 1975.

6. Weaver, W. R.; and Meador, W. E.: Values of the Photometric Parameters of Mars and Their Interpretation. NASA TM X-71949, 1974.

7. Weaver, W. R.; and Meador, W. E.: The Wavelength Dependence and an Interpretation of the Photometric Parameters of Mars. NASA TM X-73937, 1976.

TABLE I. CHEMICAL ANALYSIS OF IGNEOUS ROCKS IN THE VICINITY OF THE COLORADO BASALT TEST MATERIAL. (FROM J. GLIOZZI, MARTIN MARIETTA AEROSPACE, DENVER, CO)

SiO_2	48.2% by weight
TiO_2	0.9
Al_2O_3	16.7
Fe_2O_3	4.0
FeO	6.3
MnO	TRACE
CaO	8.3
MgO	5.8
K_2O	4.1
Na_2O	3.2
P_2O_5	0.7
Cl	0.1
H_2O+	1.7

TABLE II. CHEMICAL ANALYSIS OF DUNE MATERIAL FROM WHICH THE BASALT DUNE SAND TEST MATERIAL WAS OBTAINED. (FROM E. W. WOLFE, U. S. GEOLOGIC SURVEY, DENVER, CO)

SiO_2	47.3% by weight
Al_2O_3	16.9
Fe_2O_3	3.3
FeO	7.7
MgO	8.3
CaO	9.7
Na_2O	3.4
K_2O	0.7
TiO_2	1.6
P_2O_5	0.4
MnO	0.2
CO_2	< 0.1
H_2O+	0.1
H_2O-	0.2

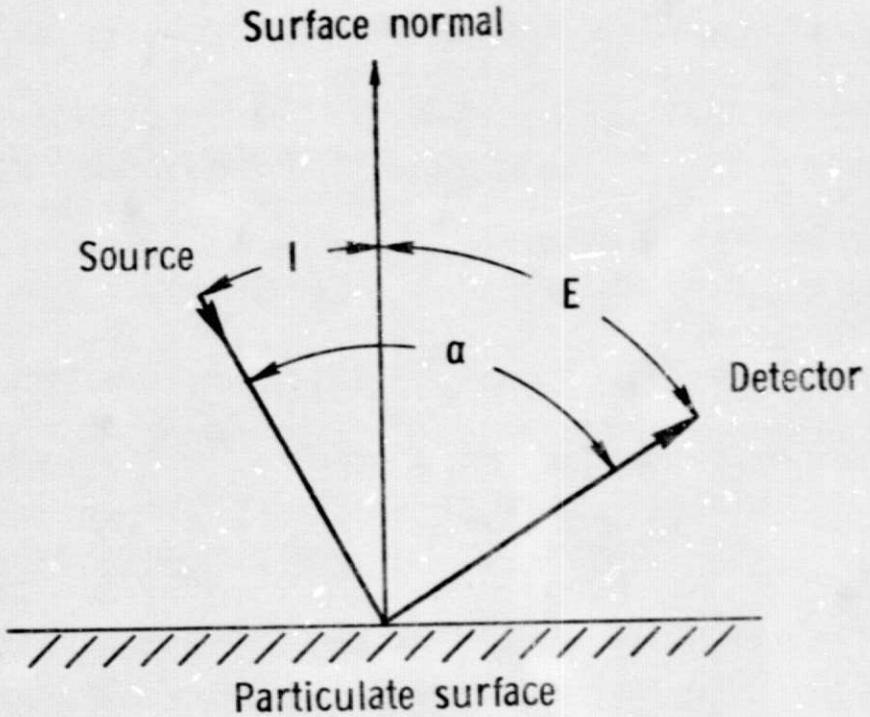

Figure 1.- Scattering geometry for photometric measurements.

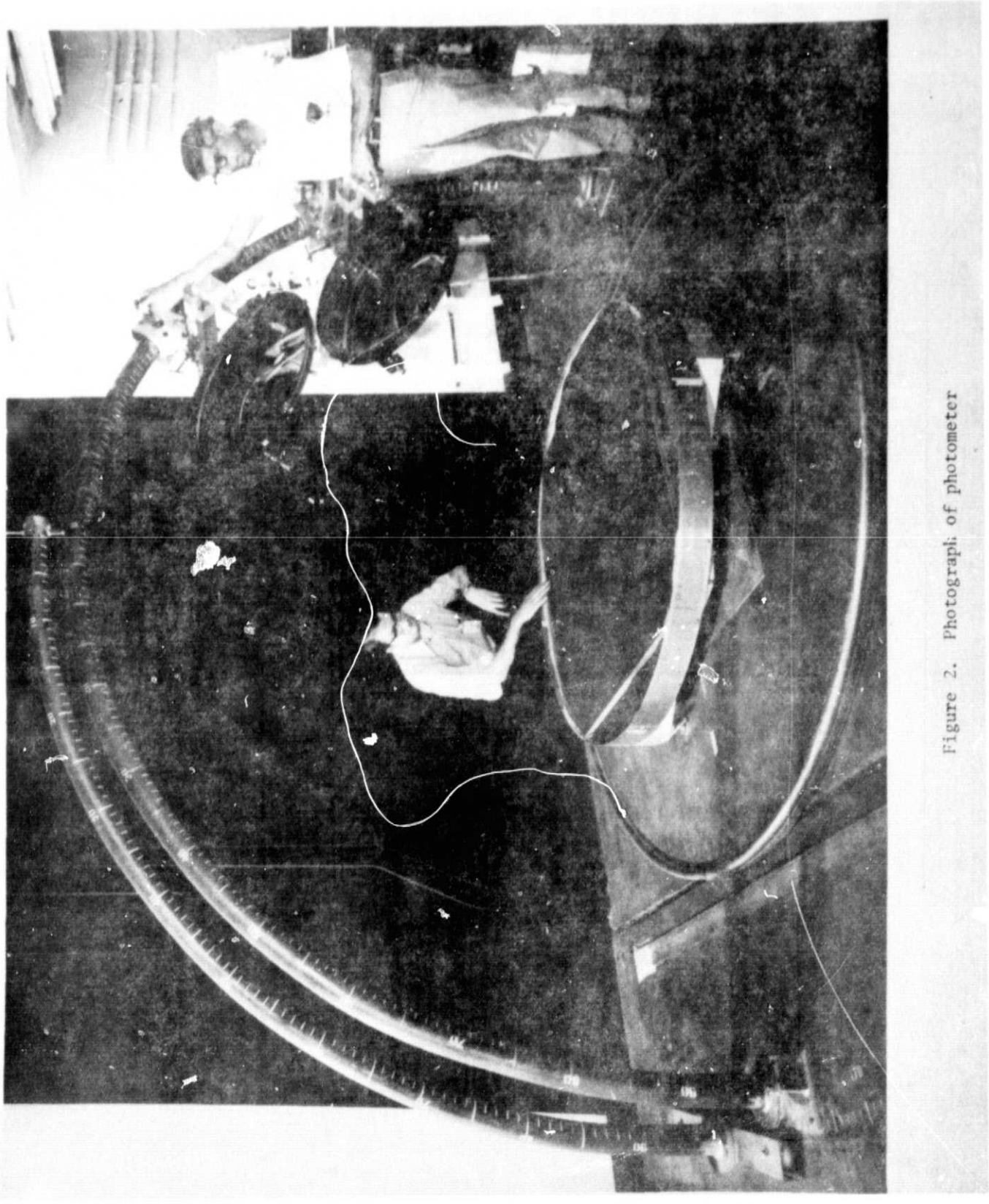

Figure 2. Photograph of photometer

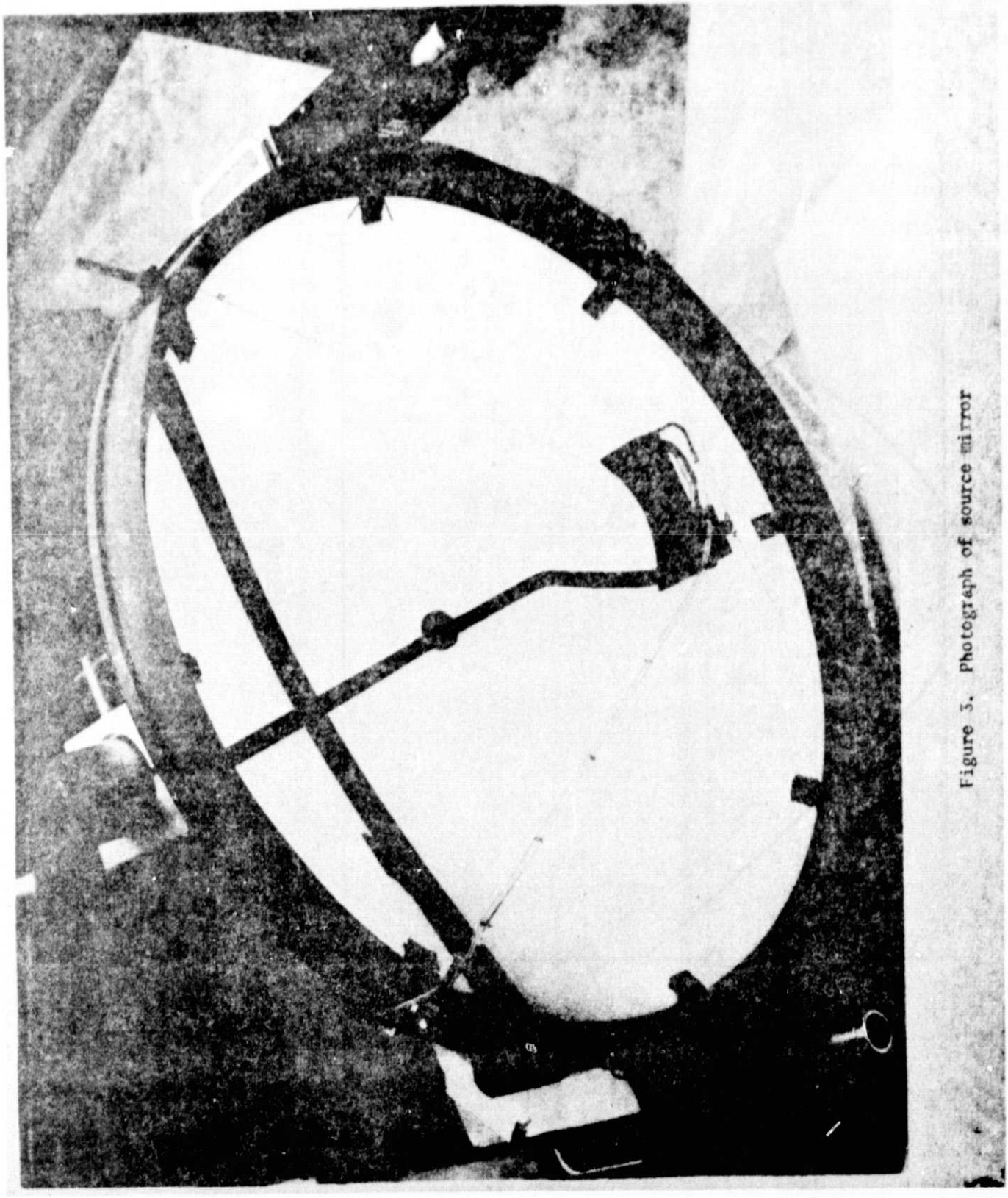

Figure 3. Photograph of source mirror

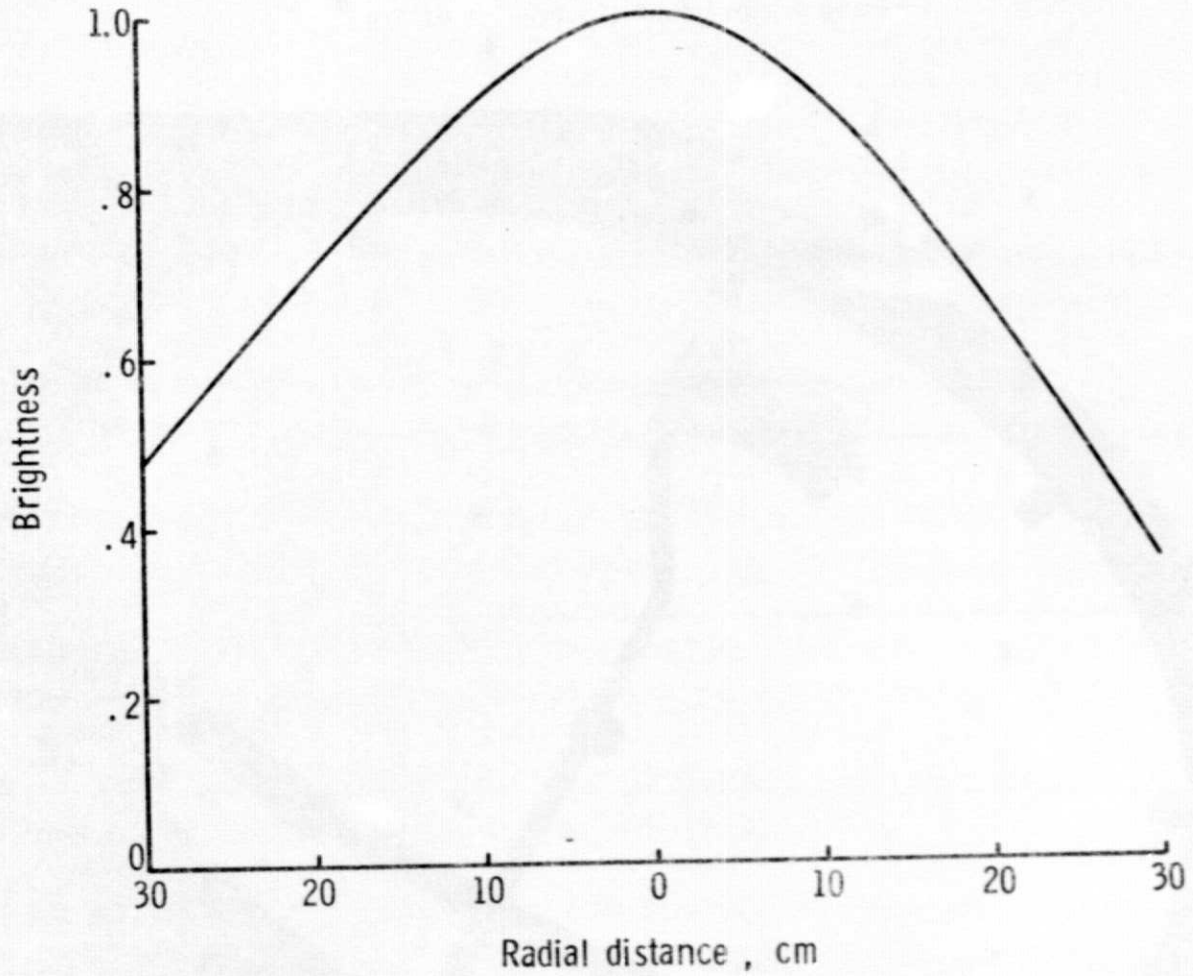

Figure 4. Source uniformity (normalized to unity at mirror's center) measured at test surface for normal incidence

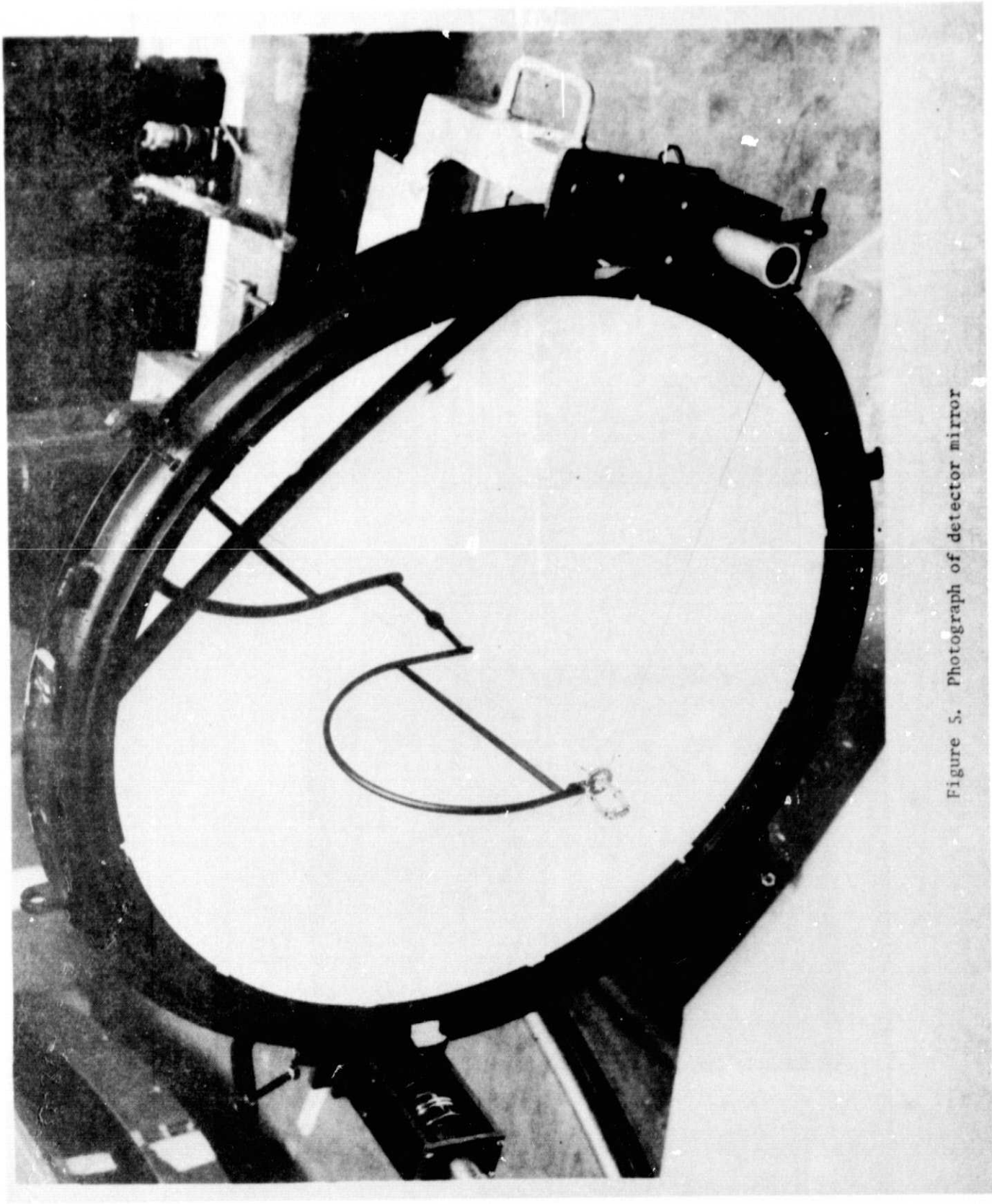

Figure 5. Photograph of detector mirror

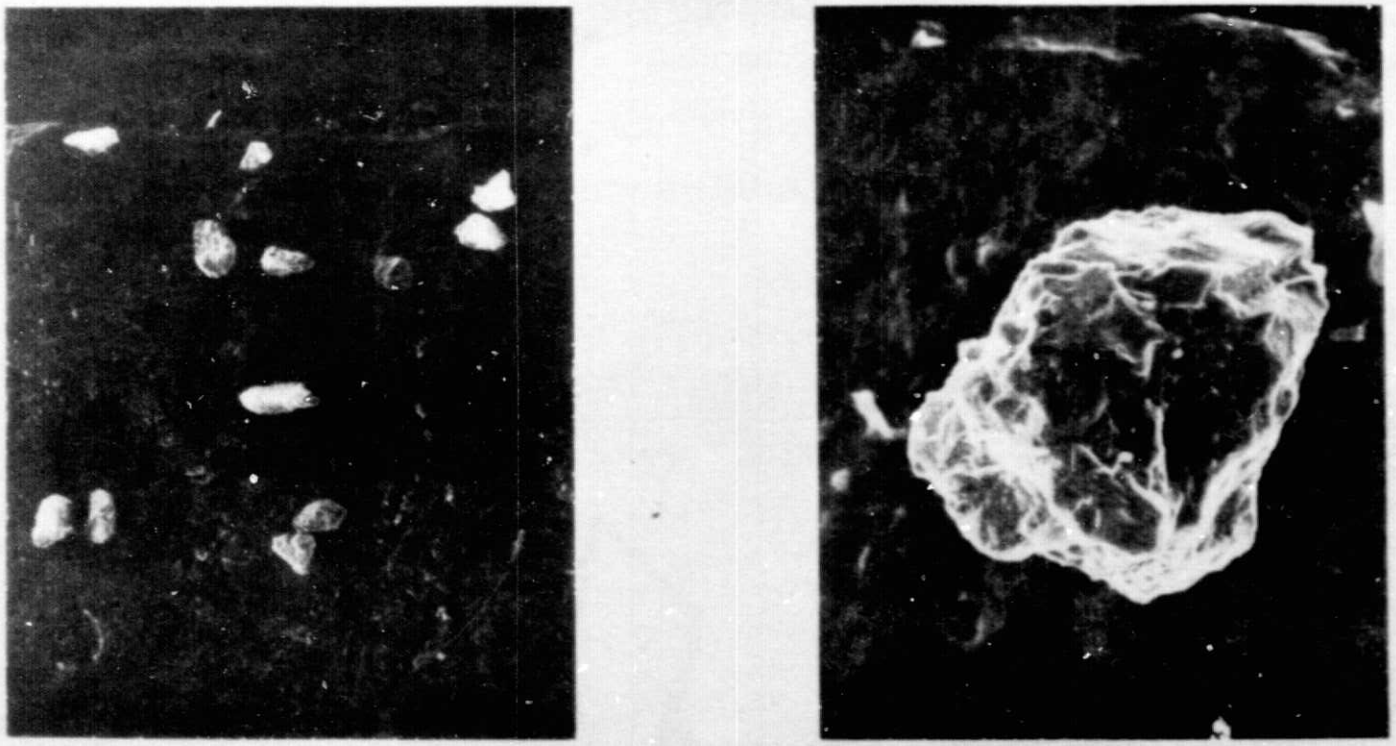

(a) (b)

Figure 6. Photographs of Colorado basalt test material taken with an electron beam microscope. Part (a) magnified 55 times and part (b) magnified 550 times.

(a)

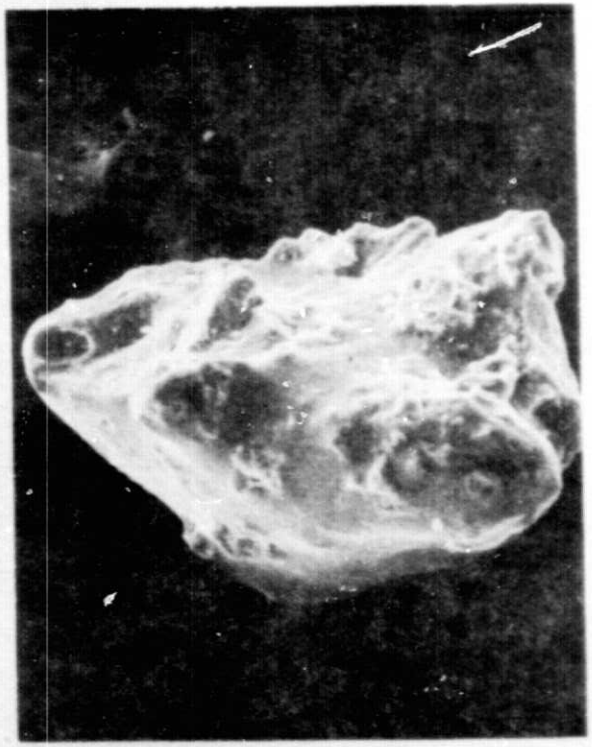

(b)

Figure 7. Photographs of basalt dune sand particles taken with an electron beam microscope. Part (a) magnified 55 times part (b) magnified 550 times.

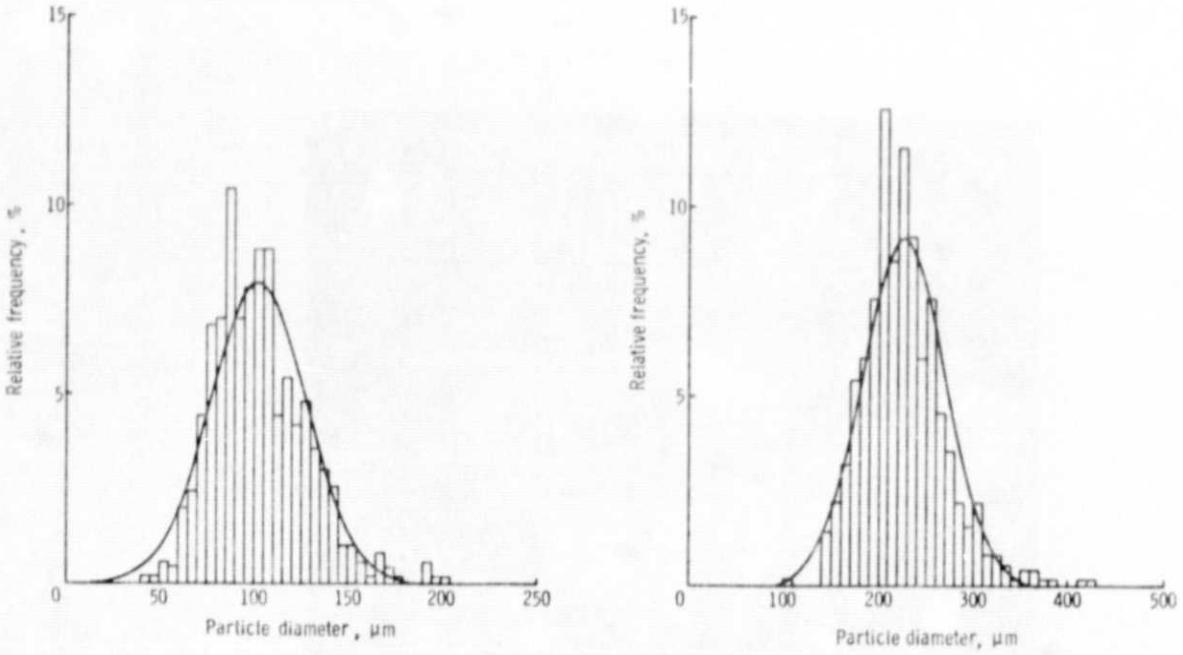

(a) Colorado basalt.

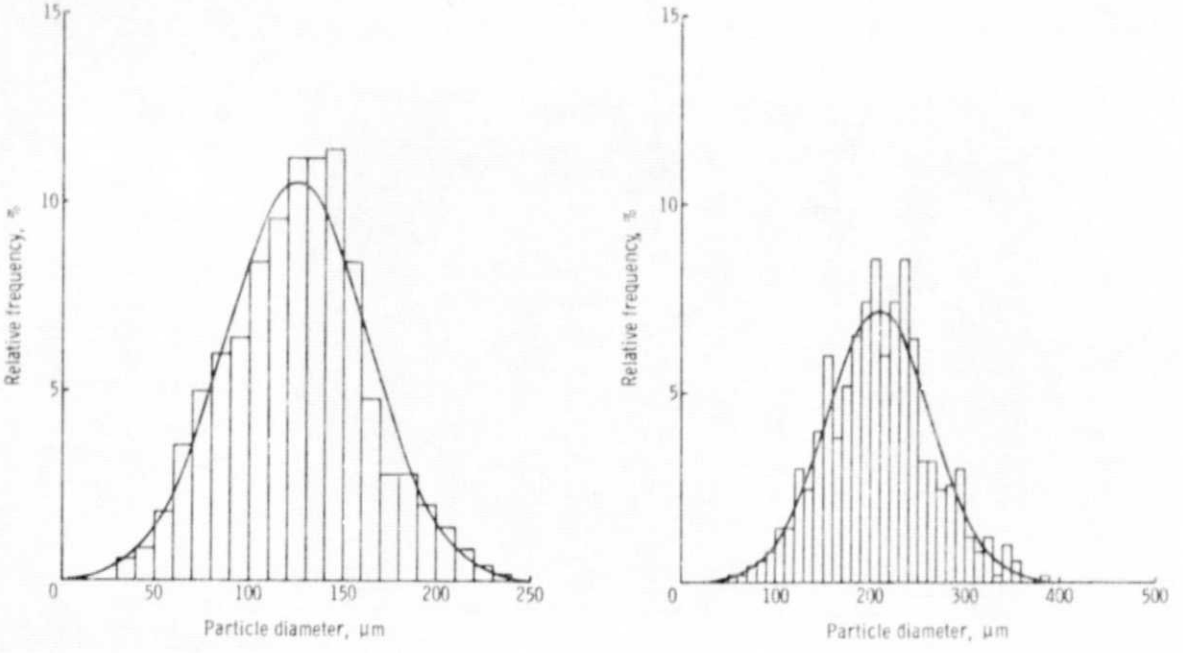

(b) Basalt dune sand.

Figure 8.- Relative frequency (number of particles per particle size increment) in percent as function of particle diameter.

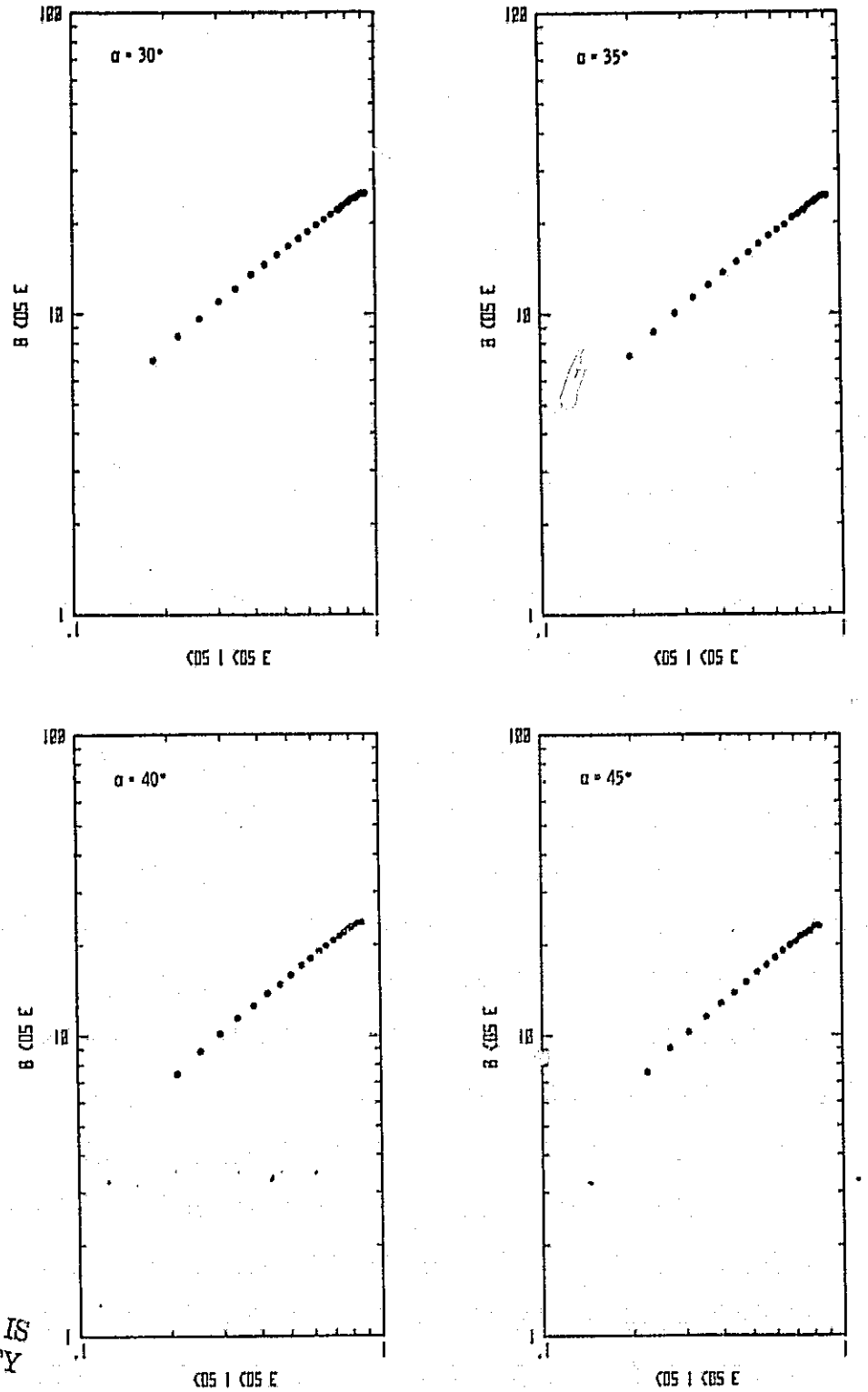

Figure 9. Minnaert plot of laboratory brightness measurements for Colorado basalt (mean particle size, 105 μm).

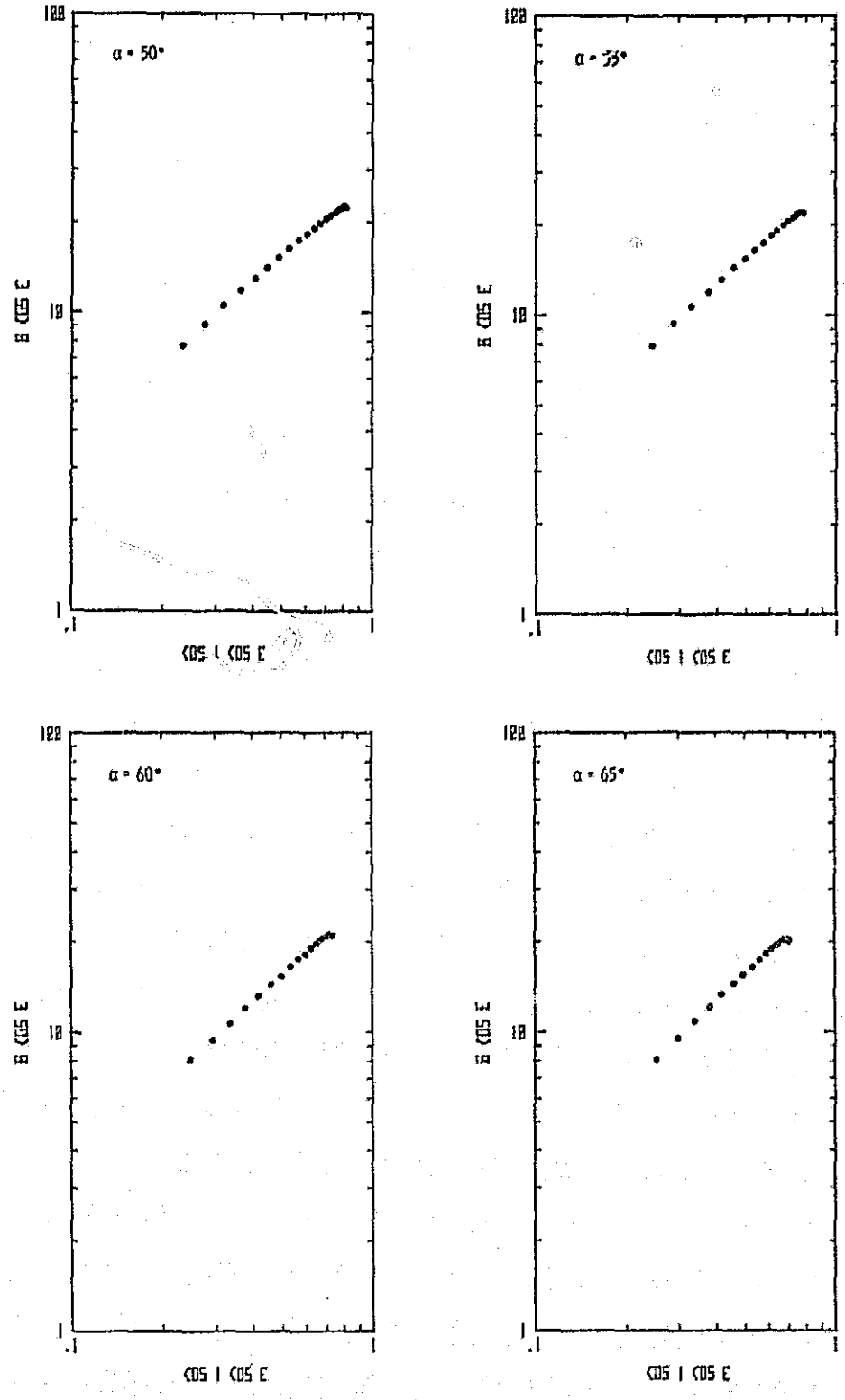

Figure 9. Continued.

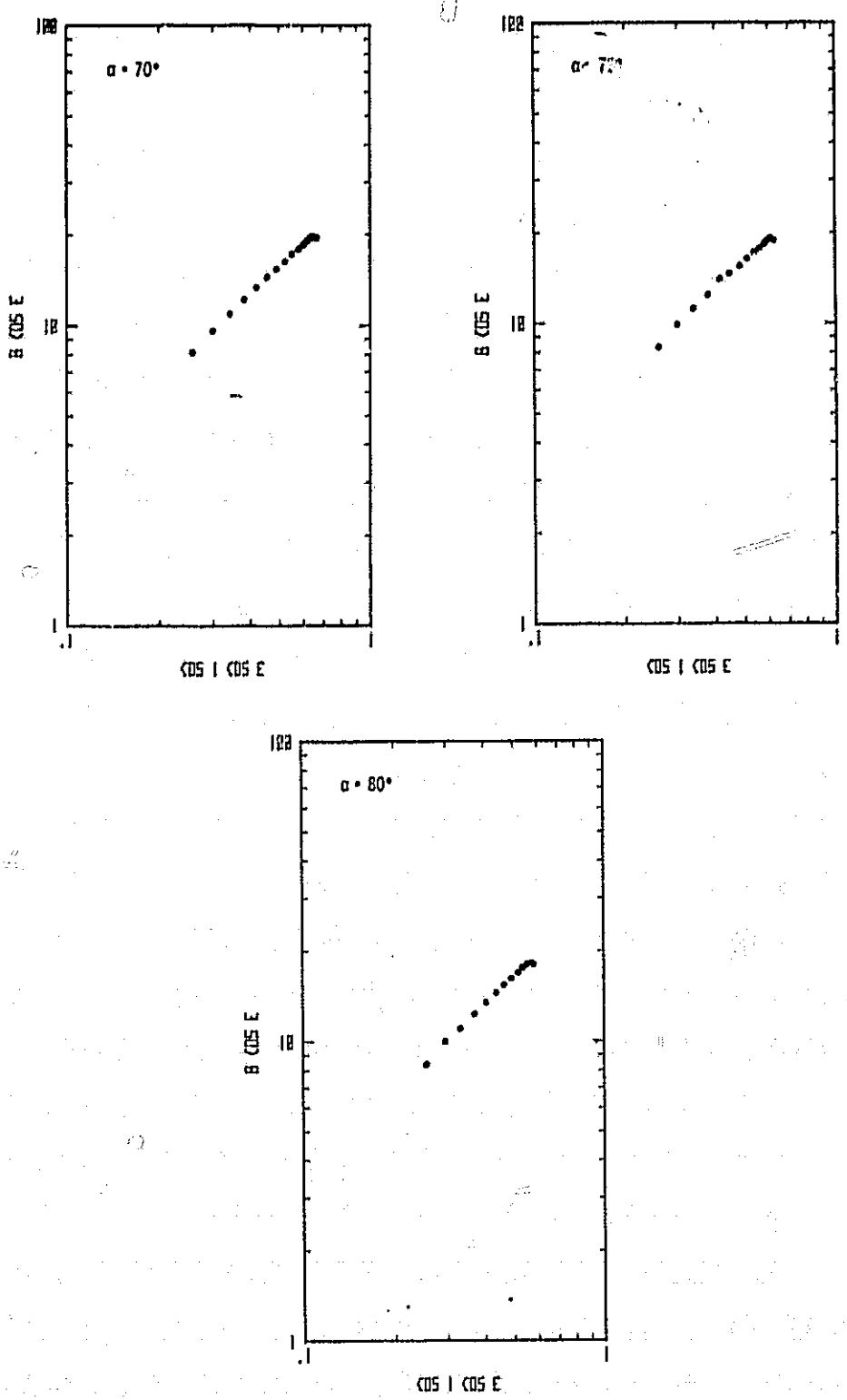

Figure 9. Concluded.

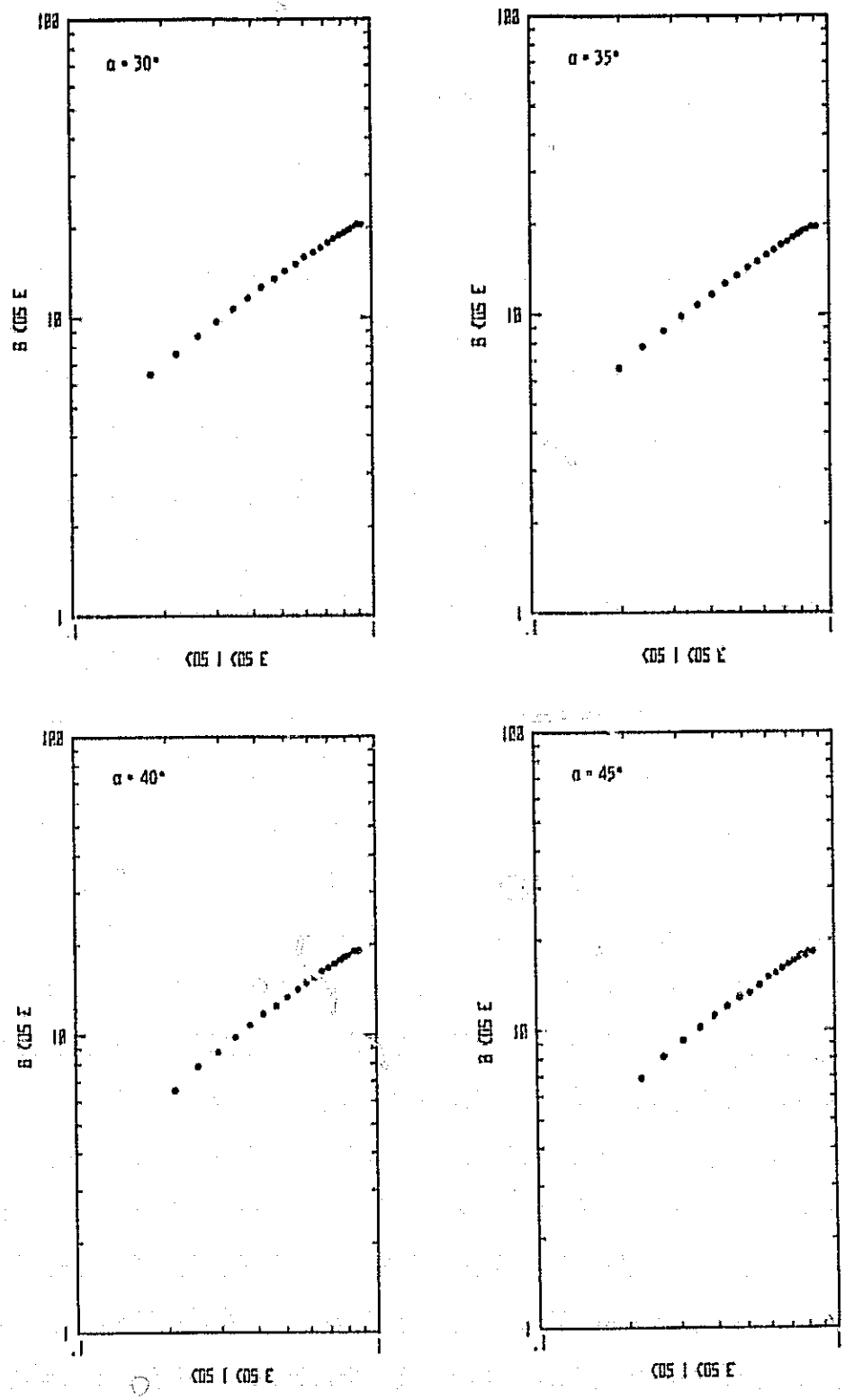

Figure10. Minnaert plot of laboratory brightness measurements for Colorado basalt (mean particle size, 225 μm).

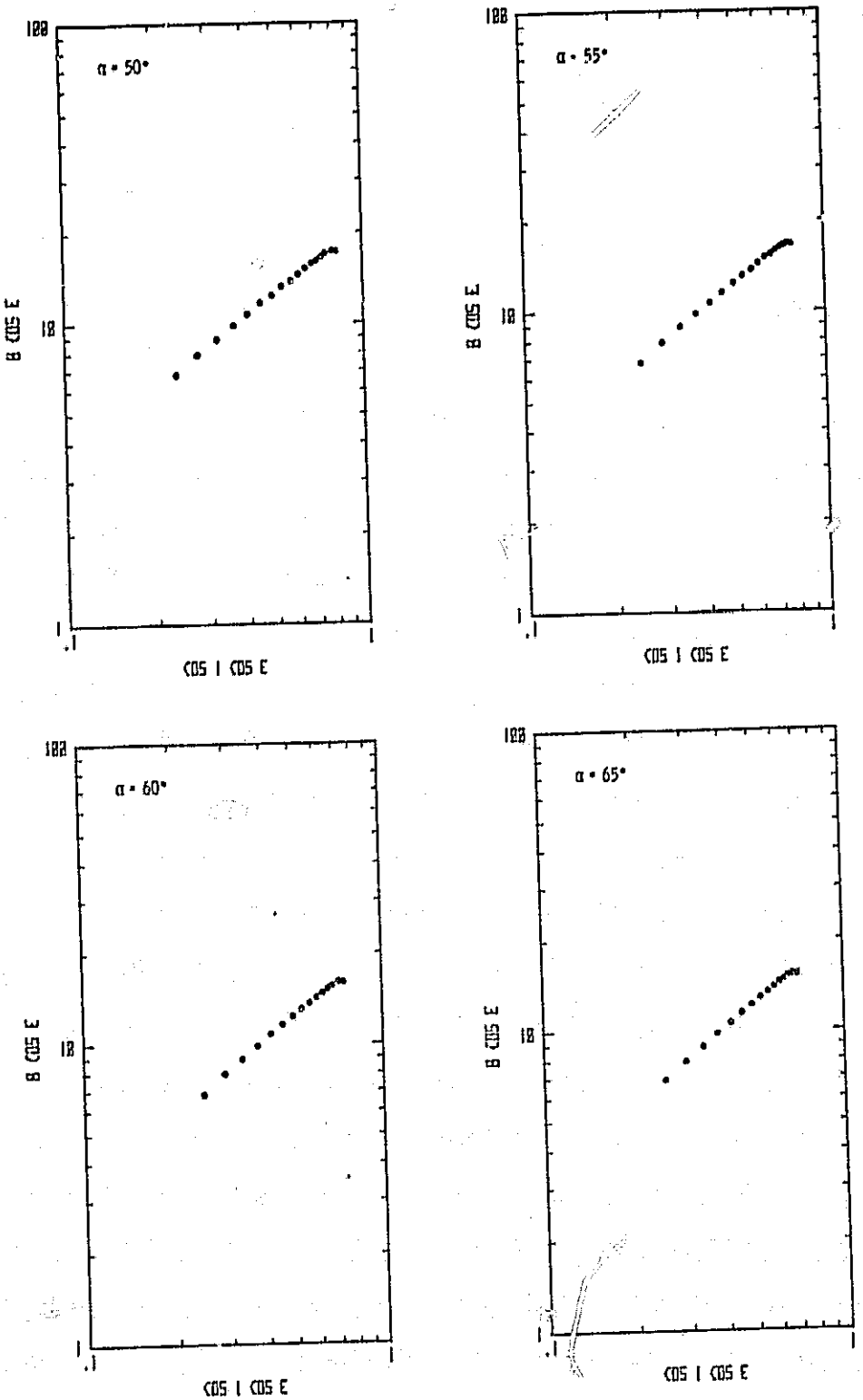

Figure 10. Continued.

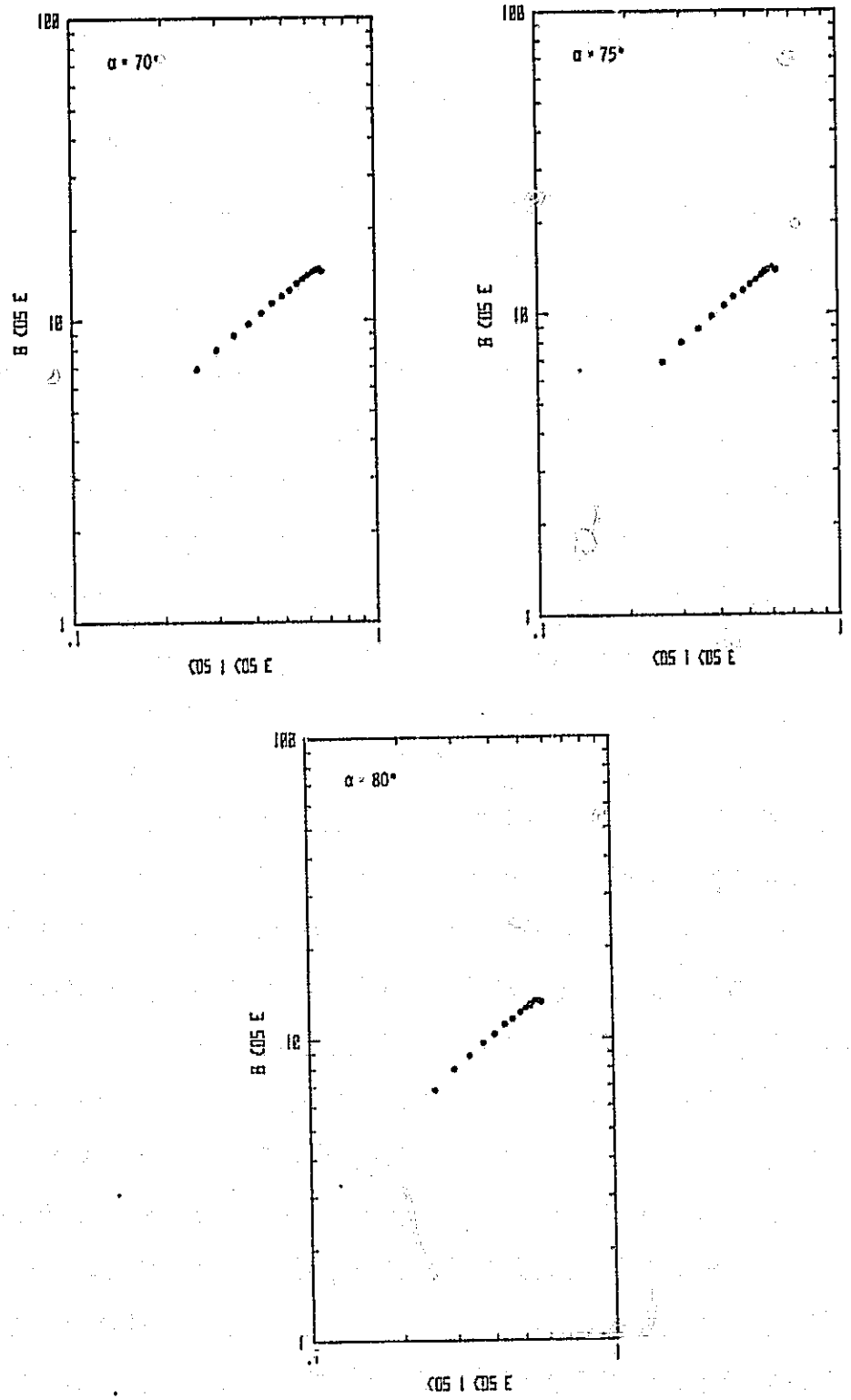

Figure 10. Concluded.

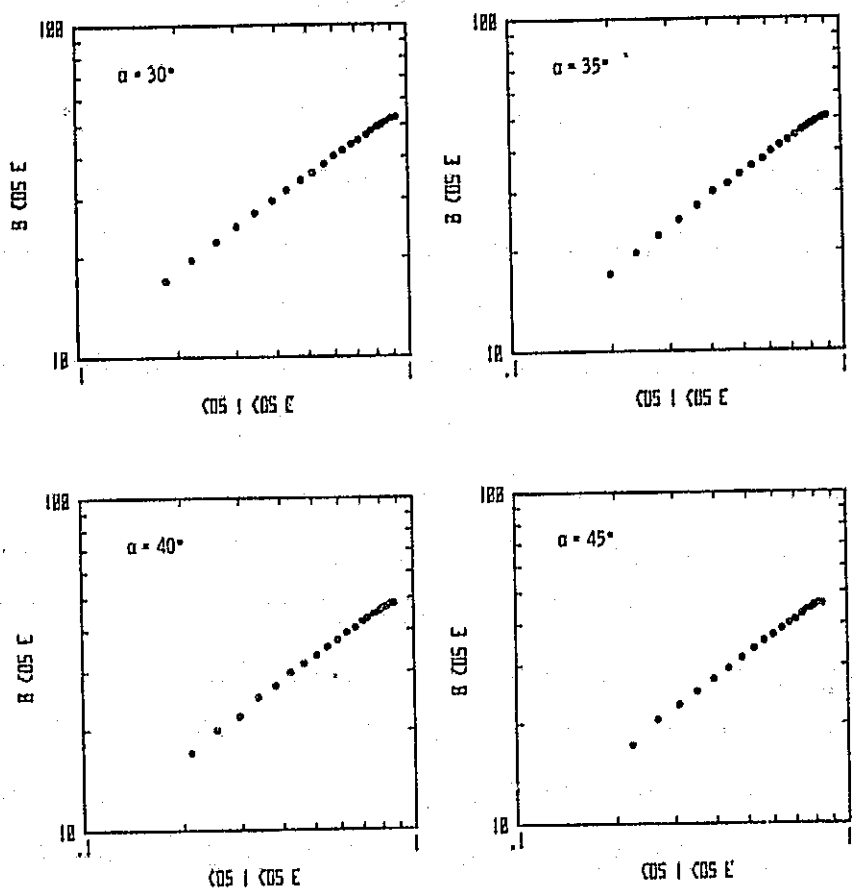

Figure 11. Minnaert plots of laboratory brightness measurements for basalt dune sand (mean particle size, 125 μm).

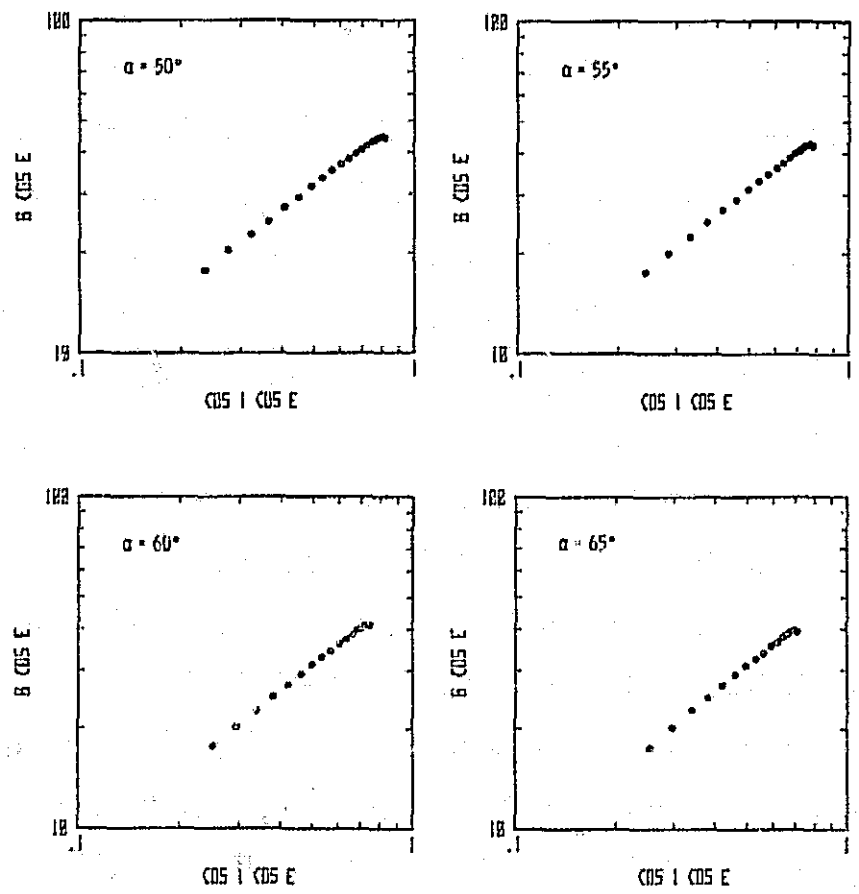

Figure 11. Continued.

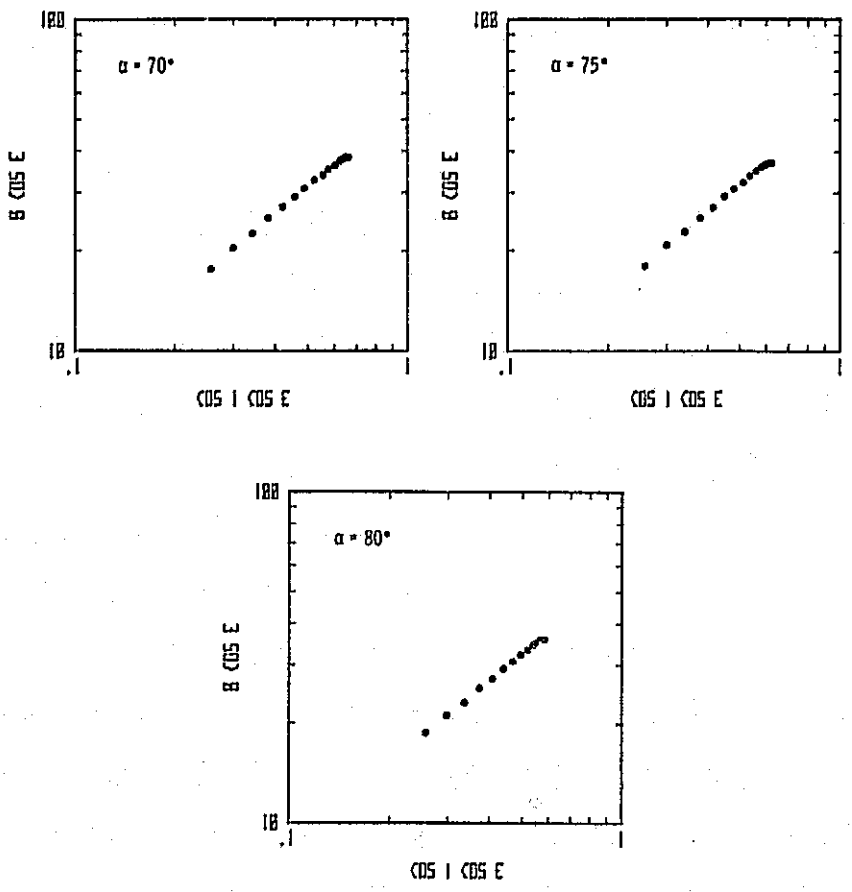

Figure 11. Concluded.

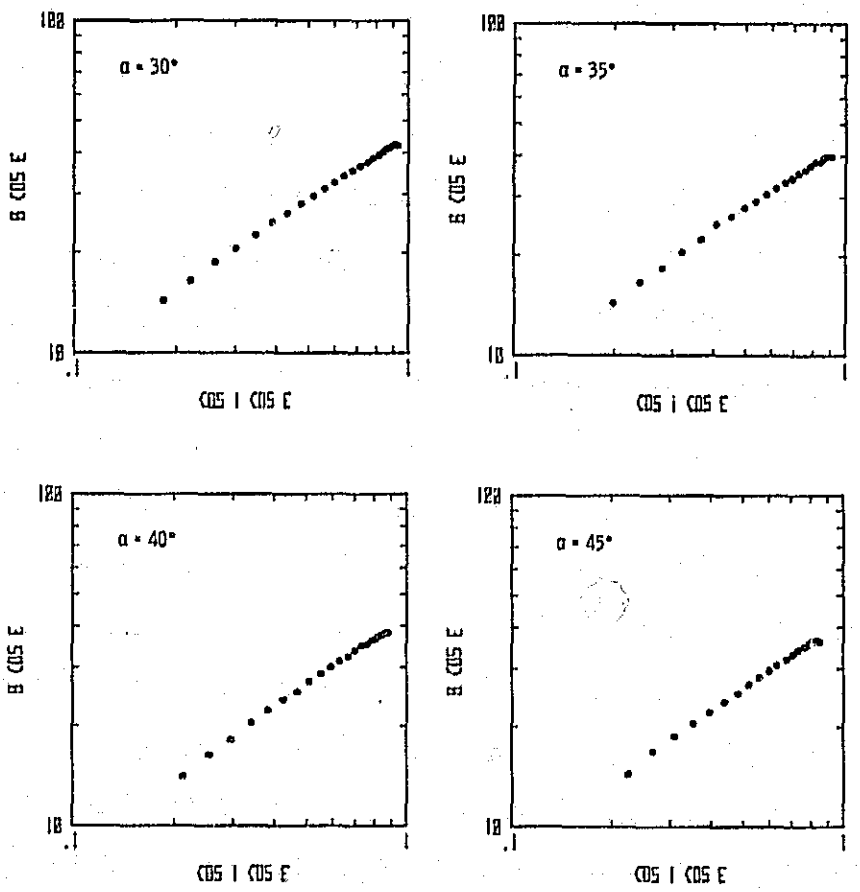

Figure 12. Minnaert plots of laboratory brightness measurements for basalt dune sand (mean particle size, 210 μm).

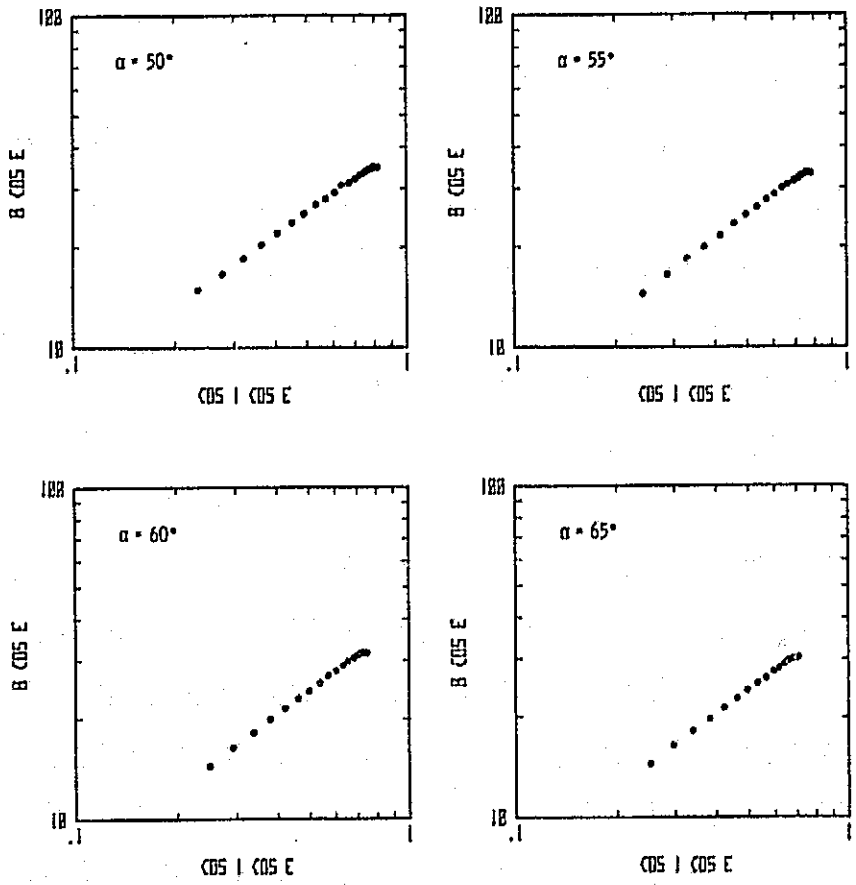

Figure 12. Continued.

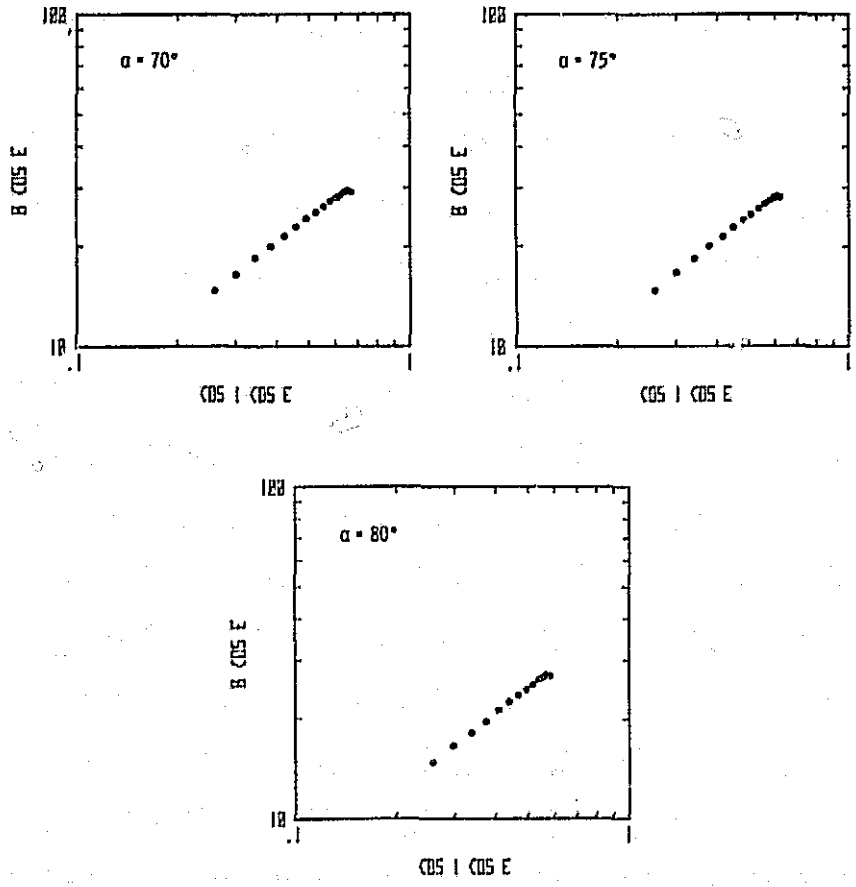

Figure 12. Concluded.

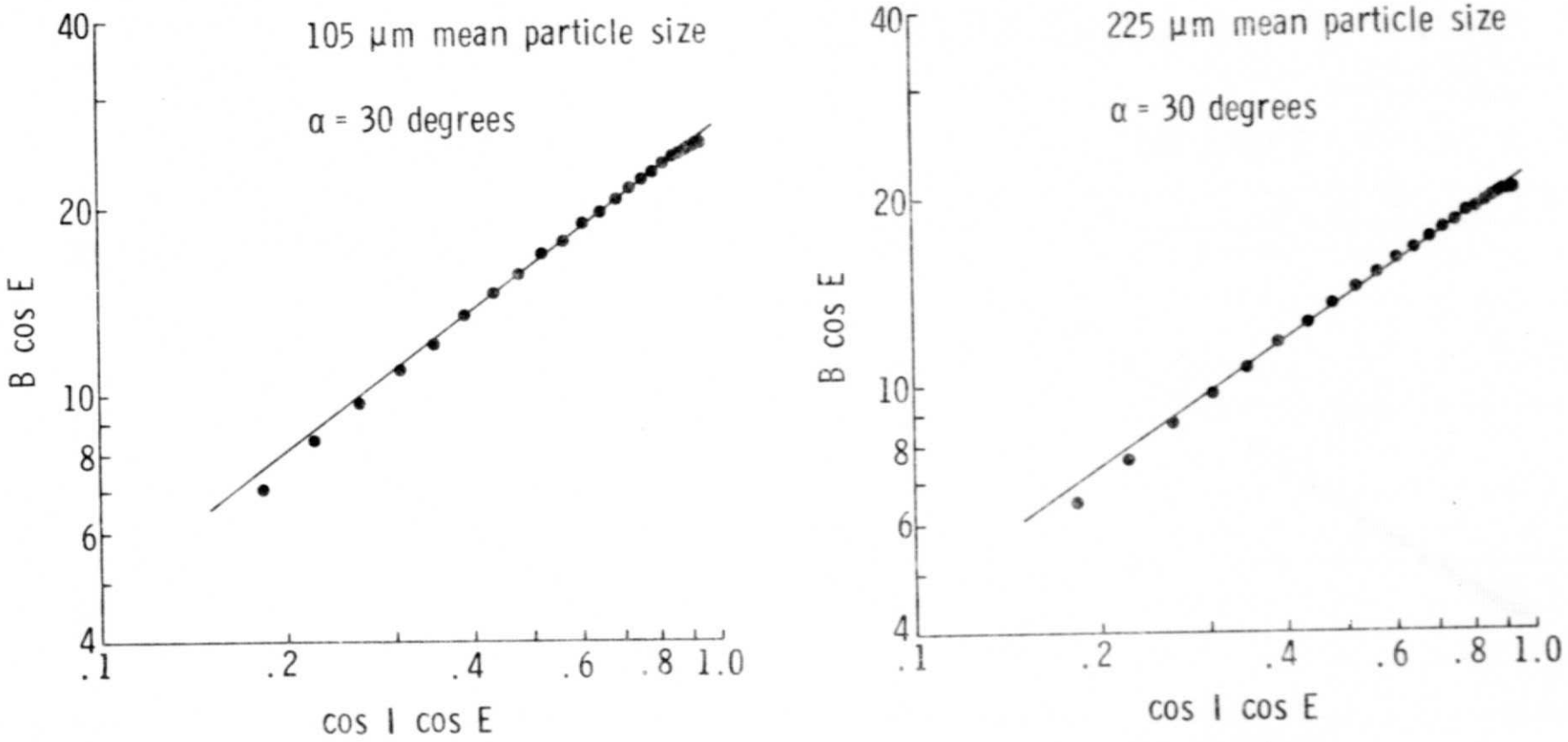

Figure 13.- Minnaert plot of laboratory brightness measurements for Colorado basalt at a phase angle of 30 degrees.

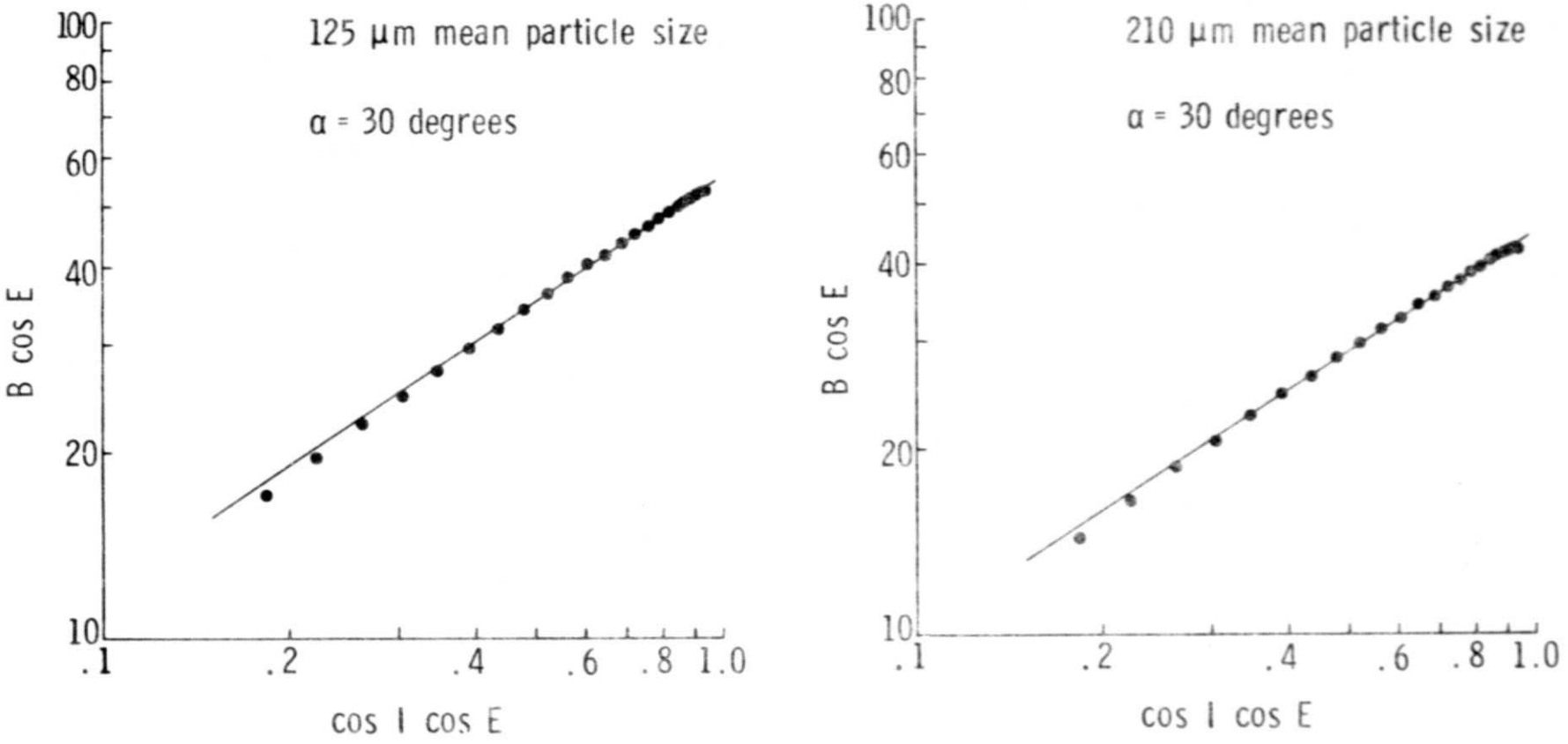

Figure 14.- Minnaert plot of laboratory brightness measurements for basalt dune sand at a phase angle of 30 degrees.